Ab Initio Cluster Model Study of the Chemisorption of CO on Low-Index Platinum Surfaces

Daniel Curulla, Anna Clotet,* and Josep M. Ricart

Departament de Química Física i Inorgànica, Universitat Rovira i Virgili, Pl. Imperial Tàrraco 1, 43005 Tarragona, Spain

Francesc Illas

Departament de Química Física i Centre de Recerca en Química Teòrica, Universitat de Barcelona, C/Martí i Franqués 1, 08028 Barcelona, Spain

Received: December 29, 1998

A systematic theoretical study of the adsorption of CO on the Pt{100}, Pt{110}, and Pt{111} surfaces is presented. The calculated equilibrium geometries and vibrational frequencies have been found to be rather independent of the cluster model chosen to represent the surface. However, calculated interaction energies are found to be very sensitive to the surface cluster model. The analysis of the chemisorption bond has been carried out by means of the constrained space orbital variation, CSOV, and of projection operator techniques. These analysis reveal that the bonding interactions are dominated by the π-back-donation although σ-donation plays a significant role. It is also clearly shown that all bonding mechanisms, other than Pauli repulsion, but specially π-back-donation, contribute to the observed red shift. However, the π-back-donation contribution to the red shift is very similar for CO on different sites. Hence, π-back-donation cannot be the mechanism responsible for the observed difference for the CO vibrational frequency on on-top and bridge sites. The CSOV decomposition reveals that the leading term contributing to this difference in vibrational frequency of chemisorbed CO is the initial Pauli repulsion or "wall effect"; this is a new, important and unexpected conclusion.

1. Introduction

The adsorption of carbon monoxide on metal surfaces has received considerable attention during the past decades. Especially, adsorption on noble metals such as rhodium, palladium, and platinum has been widely studied.[1−4] Catalysts containing such noble metals in different forms and ratio have been used widely to lower the emissions of CO, and hydrocarbons, in the automobiles exhaust.[3] These catalysts promote the oxidation of CO and C_xH_y species to CO_2 and H_2O. An additional and very important function of these catalysts is to promote the reduction of NO to N_2, via reaction of NO with hydrogen or CO. Platinum is used because of its activity on CO oxidation and, also, for hydrocarbon full oxidation. Moreover, it has been known for long time that platinum catalyses the reduction of NO_x species to N_2.[5] On the other hand, interest in carbon monoxide has increased because of its possible application to energy resources other than natural gas and petroleum; the Fischer−Tropsch reaction provides one of the key examples.[1,3,4] In any process involving gasification of hydrogen deficient materials to hydrocarbons or other organic compounds, CO is one of the main products of the gasification step, and its subsequent hydrogenation to form the required final products is of extreme importance. In addition to that, any catalytic event on a solid surface must be preceded by an adsorption step. Depending on whether physisorption or chemisorption takes place, the adsorption step significantly modifies the electronic structure of the adsorbate. Therefore, variations in the chemisorbed state might be expected to have marked effects on the reactivity of the surface species and precise information about the chemical state of adsorbed molecules is of great importance. Further, CO has been used for a long time as a probe molecule to test new experimental techniques and new theoretical methods in surface science studies.

Experimental studies about adsorption of CO on the three low index Pt surfaces covering almost all existing surface science techniques have been reported since the early days of this field.[6−46] This large body of literature is complemented with several studies about the CO oxidation and reaction with NO on Pt{100}.[47−55] This exhaustive set of references can be divided in three main groups depending on the particular crystal face involved. Thus, works on Pt{100} are grouped in refs 13 and 37−46, those dealing with Pt{110}correspond to refs 28−36 and, finally, refs 6−27 gather the works on Pt{111}. In the forthcoming discussion we will briefly describe the key features of these experimental studies with special emphasis on properties which are relevant to the present work. This summary will be given for the three low index surfaces separately starting with Pt{100}.

The clean Pt{100} surface is reconstructed at room temperature in such a way that the stable phase exhibits a (5×20) structure, referred as Pt{100}-hex by Heilmann et al.[37] The adsorption of some molecules, such as CO or NO, induces the removal of the reconstruction,[38] and a transition phase takes place from the hex structure to the ideal (1×1) bulk termination structure. This phase transition has been pointed out as the key factor in the oscillatory behavior of the CO oxidation kinetics.[47]

* Corresponding author. E-mail: clotet@quimica.urv.es. Fax: 34 977 559563.

10.1021/jp984802g CCC: $18.00
Published on Web 06/06/1999

Behm et al.[41] observed two losses in EELS experiments: a lower frequency band at 1950 cm^{-1} and a high-frequency band in the region between 2000 and 2030 cm^{-1}. They attributed these bands to the presence of bridge-bonded species and to terminal-bonded species, respectively. However, recent RAIRS experiments of CO on Pt{100}-(1 × 1)[44] do also exhibit two features in the CO frequency region, but the lower frequency appears at 1870 cm^{-1} and the higher frequency at 2067 cm^{-1}. Both bands shift to higher frequencies when the CO coverage increases. The low coverage heat of adsorption, 156 kJ/mol, has been estimated by Thiel et al.[42] from TDS experiments, whereas Yeo et al.[46] report a larger value of 215 kJ/mol from single-crystal adsorption calorimetric measurements.

The clean Pt{110} surface is also reconstructed and exhibits a (1 × 2) structure. When CO chemisorbs on this Pt{110} surface at low coverage, isolated molecules of CO on the (1 × 2) reconstructed phase coexist with islands of CO on Pt{110}-(1 × 1); upon increasing coverage, this phase transition is completed. An exhaustive study of the surface structures formed by chemisorption of CO on Pt{110} was reported by Hofmann et al. using LEED, ARUPS, and TDS.[31] Later, HREELS and RAIRS experiments by Bare et al.[32] found that only one band, at 2080 cm^{-1}, could be seen in the CO frequency region at low coverage and was attributed to CO adsorbed at on-top sites. At high coverage, $\theta > 0.5$, a second band appears at 1915 cm^{-1}, and was attributed to CO molecules adsorbed at bridge sites. Similar results were reported by Hayden et al.[33] in RAIRS experiments. However, different groups reported different values for the initial heat of adsorption. For example, Engstrom and Weinberg[34] and Fair and Madix[28] estimated a value of 150 kJ/mol, whereas Jackman et al.[29] and, more recently, Wartnaby et al.,[35] obtained a value of about 180 kJ/mol.

Unlike Pt{100} and Pt{110}, the Pt{111} surface exhibits no reconstruction. Chemisorption of CO on Pt{111} leads to a well-ordered c(4 × 2) phase, and the structure of this CO−Pt{111} phase has been accurately determined by means of quantitative LEED analysis.[20] With respect to the vibration features of CO on Pt{111}, two bands are observed also in the CO frequency region. Hayden et al.[18] observed a band at 2094 cm^{-1} assigned to the terminal-bonded CO molecules and a band at 1870 cm^{-1} for the bridge-bonded species. Similar values were reported by Hoge et al.[21] The microcalorimetric experiment carried out by Yeo et al.[27] determined a value of 183 ± 8 kJ/mol for the initial heat of adsorption of CO on Pt{111}; rather lower values, ∼120−160 kJ/mol, are reported by other authors.[9,17]

So far, we have presented a brief review of some of the, in our opinion, most significant experimental works. Now, we will turn our attention to the different theoretical approaches available in the literature. Contrary to the huge amount of experimental work devoted to CO on Pt surfaces, only a few theoretical articles concerning the interaction of CO with platinum have been published.[56−67] Ray and Anderson reported the geometries of adsorption of CO on Pt{111} and their interaction energies using a very crude approach; the atom superposition and electron delocalization, ASED, technique. The interaction energies calculated by Ray and Anderson[56] are 160 kJ/mol for the on-top site (terminal-bonded CO) and 122 kJ/mol for the bridge-bonded species. Surprisingly, these values are in good agreement with the earlier experimental values reported[9,17] but lower than the accurate measurements of Yeo et al.[27] Roszak and Balasubramanian[59] studied the triatomic Pt−CO system by using relativistic CASSCF and MRCI calculations and reported C−O (1.15 Å) and Pt−C (1.90 Å) distances which are close to the experimental ones for the CO−Pt{111} surface. Illas et al.[63,64] used the ab initio cluster model approach with a rather small four-atom model and found values of 1.13 and 2.00 Å for the C−O and Pt−C distances, respectively. These are also close to 1.16 Å and 1.85 Å, the quantitative LEED experimental values reported by Ogletree et al.[20] The calculated Pt−C distance is too large and additional calculations have found that the origin of this discrepancy lies in the use of a large core pseudopotential.[65] More recently, a theoretical study for the Pt{100} surface has been reported by Pacchioni et al.,[67] also using small cluster models but all-electron basis sets for Pt. They showed that relativistic effects play a very important role in the geometry of the adsorbed species. No theoretical works about CO on Pt{110} have been found. For an exhaustive description of ab initio adsorbate/cluster model calculations the reader is referred to the recent review by Whitten and Yang.[85]

In this work we present a systematic theoretical study of the adsorption of CO on Pt{100}, Pt{110}, and Pt{111} surfaces. This study has been encouraged by the limited structural information available for the CO adsorption on Pt{100} and Pt{110}, and by the lack of theoretical information, which does not allow a complete understanding of the interaction of CO on the different platinum surfaces. Detailed studies of adsorption of CO on single-crystal surfaces, geometry of adsorbed molecules, vibrational frequencies, and bonding properties at different sites and at various coverages are necessary for the comprehension of the adsorption properties of CO on metals or more complex catalysts. This work attempts to provide a further step toward understanding the interaction, structure, and vibration features of CO on low index Pt surfaces.

2. Cluster Models and Computational Details

The ab initio cluster model approach has been used to study the adsorption of CO on the low-index platinum surfaces. Several cluster models have been designed to describe the interaction of carbon monoxide with the three different surfaces studied on various adsorption sites. For the Pt{100} surface, on-top, bridge, and 4-fold hollow sites have been analyzed. A five-atom cluster model, with one atom at the first layer and the rest in the second layer, has been used for the on-top site and we will denote it as Pt_5(1,4). An eight-atom cluster model, with two atoms in the first layer and six in the second one, has been used for the bridge site, Pt_8(2,6). Again, a five-atom cluster model has been used for the 4-fold hollow site, but now with four atoms in the first layer and only one in the second, Pt_5(4,1). We have also built up a 29 atom cluster model, Pt_{29}(16,9,4), that permits us to study the three adsorption sites with the same cluster and makes possible a direct comparison of the results obtained for the different adsorption sites and, also, to investigate possible cluster size effects. The cluster models for the Pt{100} surface are shown in Figure 1. In the case of Pt{110} we have analyzed the adsorption at on-top and short-bridge sites. The cluster models used are Pt_5(1,4), for the on-top site, Pt_8(2,6), for the bridge site, and Pt_{29}(16,9,4), for both sites (Figure 2). Finally, in the case of Pt{111}, only the adsorption at on-top and bridge sites has been investigated because there is no evidence that a 3-fold adsorption may occur. For this surface, the clusters used are Pt_4(1,3), for the on-top site, Pt_5(4,1), for the bridge site, and the larger Pt_{25}(14,8,3), used to study both adsorption sites (Figure 3). For all cluster models, the positions of the atoms have been fixed as in bulk platinum, with a lattice parameter of 3.9239 Å leading to a nearest-neighbor Pt−Pt distance of 2.7746 Å. We will show that, as expected, local properties such as equilibrium geometries and

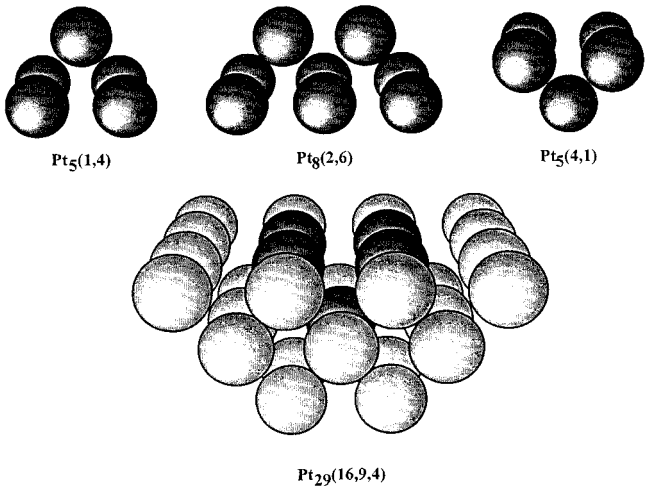

Figure 1. Cluster models used to simulate the on-top site, the bridge site, and the 4-fold hollow site of the Pt{100} surface.

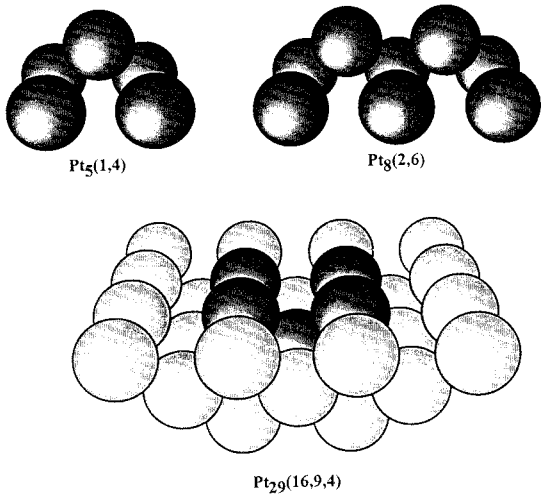

Figure 2. Cluster models used to simulate the on-top site and the bridge site of the Pt{110} surface.

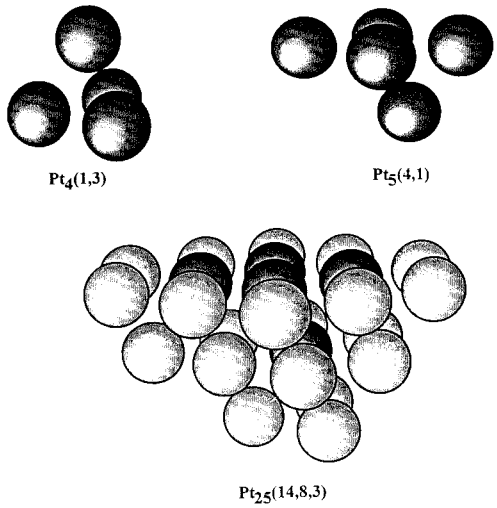

Figure 3. Cluster models used to simulate the on-top site and the bridge site of the Pt{111} surface.

vibrational frequencies can be well reproduced even by the small cluster models. This assumption was demonstrated by Bauschlicher et al. refs 86 and 87 and references therein who have shown that geometrical parameters and vibrational frequencies converge quite fast with respect to cluster size. Further, we have employed these small models to analyze the bonding mechanism and to decompose the vibration shift into several contributions. We would like to point out that recent work involving CO on Pt(111) cluster models has shown that these contributions are rather independent of the size of the cluster model used to represent the surface.[64]

Following recent work,[65] we have used the Hay-Wadt relativistic effective core potential, ECP, which explicitly includes the $5s^25p^65d^{10}$ electrons, for all the platinum atoms in the small cluster models, and the basis set used for these atoms is the double-ζ one recommended by Hay-Wadt.[68] In the large cluster models, we can distinguish two different kinds of atoms, those corresponding to the local region that defines the adsorption site and the rest of the platinum atoms. The atoms in the local region have been described with the small core Hay-Wadt ECP, whereas the remaining, environmental, atoms have been described with a one-electron ECP[69] within a double-ζ basis set. Both the carbon and the oxygen atoms have been described with the standard 6-31G* basis set. More precisely, the $Pt_{29}(16,9,4)$ cluster models have five atoms described with the Hay-Wadt small core ECP, four in the first layer, and one in the second, and the remaining 24 atoms are described with the one-electron ECP. In the case of the $Pt_{25}(14,8,3)$ cluster model, four atoms in the first layer, and only one in the second layer have been described with the small core Hay-Wadt ECP; again the rest of atoms in the cluster are described with the help of the one-electron ECP.

Ab initio Hartree−Fock and B3LYP hybrid density functional theory calculations have been carried out using HONDO8.5[70] and Gaussian94[71] computational packages. Properties such as binding energies, vibrational frequencies, and geometrical parameters, shown in the following section, have been calculated within the B3LYP exchange-correlation functional whereas Hartree−Fock wave functions have been used to analyze the chemisorption bond, section 4. Binding energies have been always corrected for the basis set superposition error, BSSE, using the counterpoise method proposed by Boys and Bernardi.[72]

3. Adsorption Geometries, Vibrational Frequencies, and Binding Energies

3.1. CO on Pt{100}. The adsorption geometries, vibrational frequencies, and binding energies for CO interacting with the cluster models defined in the previous section have been computed at the B3LYP level of theory and results are summarized in Table 1. The binding energies calculated with the small cluster models are 178 kJ/mol for the CO adsorbed at on-top sites, 244 kJ/mol for the bridge-bonded CO molecules, and 98 kJ/mol for the CO adsorption at 4-fold hollow sites. The initial heat of adsorption reported by Thiel et al., from TDS experiments, is 156 kJ/mol[42] and much larger value of 215 kJ/mol was reported recently by Yeo et al.[46] through single-crystal adsorption calorimetric measurements. The experimental work assumes that the heat of adsorption at both on-top sites and bridge sites is very similar. This assumption is supported by the fact that, at low coverage, adsorption at on-top sites as well as at bridge sites is found and that no sequential filling is observed. From our results on the small cluster models one would deduce that adsorption at bridge sites is largely favored compared to adsorption at on-top sites. However, comparison between the two adsorption sites is not straightforward because different cluster models were used to model the different sites. It is well-known that the binding energy is the property that depends most on the size and the topology of the cluster model. Therefore, a cluster model able to describe both adsorption sites has to be used if one wishes to compare the heat of adsorption

TABLE 1: Binding Energies, Geometrical Parameters, and Vibrational Frequencies for the CO Chemisorbed on Pt{100}[a]

	B.E. (kJ/mol)	d_{CO} (Å)	d_{S-CO} (Å)	d_{PtC} (Å)	ν_{CO} (cm^{-1})	ν_{PtCO} (cm^{-1})	$\Delta\nu_{CO}$ (cm^{-1})
			On-Top				
Pt_5(1,4)	178	1.158	1.865	1.865	2064	454	−147
Pt_{29}(16,9,4)	132	1.154	1.870	1.870	2087	454	−124
			Bridge				
Pt_8(2,6)	244	1.183	1.398	1.969	1881	401	−330
Pt_{29}(16,9,4)	127	1.174	1.490	2.036	1925	339	−286
			4-Fold Hollow				
Pt_5(4,1)	98	1.204	1.046	2.223	1707	301	−504
Pt_{29}(16,9,4)	70	1.185	1.256	2.330	1808	232	−403

[a] B.E. is the binding energy calculated as $-[E(\text{cluster} + \text{CO}) - E(\text{cluster}) - E(\text{CO})]$, d_{CO} is the C−O distance, d_{S-CO} is the height of the CO molecule from the surface, d_{PtC} is the Pt−C distance, ν_{CO} is the CO stretching frequency, ν_{PtCO} is the PtC stretching frequency, and $\Delta\nu_{CO}$ is the CO stretching frequency shift calculated as $\nu_{CO} - \nu_{CO,free}$, where $\nu_{CO,free}$ is the computed CO stretching frequency of the free CO molecule.

at different sites. A possible cluster model is precisely Pt_{29}-(16,9,4). With this larger cluster model, a binding energy of 132 kJ/mol is obtained for terminal-bonded CO and 127 kJ/mol for bridge-bonded CO. First, we notice that, as expected, both sites have similar heats of adsorption, the on-top sites being slightly favored in agreement with experimental studies. Second, these values are much smaller than those arising from the small cluster models. This is specially true for the bridge site, showing once again that the binding energy strongly depends on the cluster size. Notice that the cluster ground state is always used here to compute the adsorbate−surface binding energies. We must mention that other possibilities exists; in particular, Siegbahn et al.[88] have shown that it is possible to obtain binding energies which are stable with respect to cluster size when the cluster electronic state is chosen according to a series of rules that lead to the concept bond prepared clusters. However, we must also remark that CSOV analysis of the interaction of CO with Cu_5 on different electronic states bond prepared or not does not reveal significant changes in the bonding mechanism except on the initial Pauli repulsion.[89] In any case, the binding energies calculated with the Pt_{29} cluster model are quite close to the value reported by Thiel et al.[42] However, a substantial difference exists between our values and the accurate measurements reported by Yeo et al.[45,46] Nevertheless, present results are in good agreement with those recently reported by Pacchioni et al.:[67] 141 kJ/mol for the on-top sites and 125 kJ/mol for the bridge sites. Since the B3LYP interaction energies are usually quite accurate, the difference with respect to experiment must be ascribed to two possibilities: the relaxation of the binding sites are not considered and the limited representation of the metal conduction band.

For adsorption at 4-fold hollow sites, the present results permit to conclude that adsorption at this site is strongly unfavored compared to adsorption at on-top and bridge sites. This conclusion arises from the fact that the binding energy for the 4-fold hollow site in the large cluster is 70 kJ/mol, more than 50 kJ/mol smaller than for the calculated values for the on-top and bridge sites obtained from the same cluster at the same level of theory. To our knowledge, no information about adsorption at 4-fold hollow sites exists in the literature. The only mention of CO 4-fold adsorption has been given by Hong and Richardson[51] who state that coadsorption with oxygen could lead the CO molecules to occupy the less favorable 4-fold hollow site.

The CO stretching frequency for the terminal-bonded CO, computed using the small cluster model, is 2064 cm^{-1}, whereas a value of 2087 cm^{-1} is obtained from the large cluster. The calculated vibrational frequency for the bridge-bonded CO is 1881 cm^{-1} with the small cluster model and 1925 cm^{-1} with the large one. The values predicted by the two different clusters differ by 23 or 44 cm^{-1} only, this is ∼2% effect. The IRAS experiments for low coverage CO adsorption on Pt{100}-(1 × 1) at 300 K gives rise to two bands, one at 2067 cm^{-1}, ascribed to terminal-bonded species, and another at 1870 cm^{-1}, attributed to bridge-bonded species.[44] The agreement between the experimental and calculated frequencies is reasonably good. However, the large cluster model leads to slightly larger vibrational frequencies, specially in the case of the adsorption at bridge sites. In any case, the difference between the calculated frequency and the experimental center of the band is 55 cm^{-1} only. Part of the difference with respect to experiment effect arises from the fact that the calculated frequencies do not include anharmonic effects. Nevertheless, the concordance between calculated and experimental values is acceptable and lies within the experimental range of values obtained from different techniques and quite similar but not identical conditions. In fact, Behm et al.[41] had previously observed a band at 1950 cm^{-1} in EELS experiments, assigned to bridge-bonded CO molecules and mentioned that adsorption on Pt{100}-hex gave rise to the same vibrational features; moreover, they did not report any change in the vibrational frequencies when increasing the coverage. On the other hand, Martin et al.[44] also reported a vibrational frequency of 1910 cm^{-1} ascribed to bridge-bonded species. A possible interpretation of the discrepancy between these two experimental measures is that both bands in the region between 1850 and 1920 cm^{-1} can be attributed to bridge-bonded CO molecules, but the bonds reflect a slightly different environment of the CO molecules.

For the adsorption at 4-fold hollow sites, the small cluster gives rise to a frequency of 1707 cm^{-1} whereas the large one leads to a value of 1808 cm^{-1}. Again, we notice that, in general, the large cluster predicts vibrational frequencies which are higher than those predicted from the small model. We remark that differences between results for the small and the large clusters grow up when high-coordinated adsorption sites are considered. Unfortunately, there is not any experimental reference for the adsorption of CO at 4-fold hollow sites in the literature and, consequently, it is not possible to check these results. Nevertheless, it is reasonable to expect that the adsorption of CO at 4-fold hollow sites would give rise to a band in the 1700 and 1750 cm^{-1} region.

Up to now, we have commented on our results for the CO stretching frequency. To close the discussion on vibration frequencies we will comment the Pt−C, frustrated translational, stretching frequencies. In the case of the adsorption of CO at on-top sites, a frequency of 454 cm^{-1} has been obtained using both small and large clusters. Values of 401 cm^{-1} with the small cluster and 339 cm^{-1} with the large one have been obtained for the adsorption of CO at bridge sites. These results agree very well with those reported by Pacchioni et al.[67] which are 464 and 339 cm^{-1} for the terminal-bonded CO and the bridge-bonded species, respectively. No experimental data about the Pt−C frequencies have been found in the literature for CO on Pt{100}. Finally, the adsorption of CO at 4-fold hollow sites gives rise to a value of 301 cm^{-1} for the small cluster model and 232 cm^{-1} for the large one. The larger differences for the Pt−C frequencies at this 4-fold site are a consequence of the very limited representation of this surface site achieved by the

TABLE 2: Same as Table 1 for the CO Chemisorbed on Pt{110}

	B.E. (kJ/mol)	d_{CO} (Å)	d_{S-CO} (Å)	d_{PtC} (Å)	ν_{CO} (cm^{-1})	ν_{PtCO} (cm^{-1})	$\Delta\nu_{CO}$ (cm^{-1})
			On-Top				
Pt_5(1,4)	139	1.153	1.825	1.825	2109	505	−102
Pt_{29}(16,9,4)	150	1.155	1.863	1.863	2082	459	−129
			Bridge				
Pt_8(2,6)	168	1.172	1.453	2.009	1941	379	−270
Pt_{29}(16,9,4)	68	1.179	1.451	2.008	1933	343	−278

TABLE 3: Same as Table 1 for the CO Chemisorbed on Pt{111}

	B.E. (kJ/mol)	d_{CO} (Å)	d_{S-CO} (Å)	d_{PtC} (Å)	ν_{CO} (cm^{-1})	ν_{PtCO} (cm^{-1})	$\Delta\nu_{CO}$ (cm^{-1})
			On-Top				
Pt_4(1,3)	229	1.157	1.852	1.852	2081	472	−130
Pt_{25}(14,8,3)	110	1.152	1.907	1.907	2098	409	−113
			Bridge				
Pt_5(4,1)	126	1.184	1.377	1.955	1874	415	−337
Pt_{25}(14,8,3)	24	1.184	1.445	2.003	1860	379	−351

small Pt_5(4,1) cluster where there is not a single cluster atom with a minimal coordination.

We will complete the discussion about adsorption of CO on Pt{100} by discussing the calculated geometrical parameters. Notice that, again, no experimental data can be found in the literature. The CO distance for the terminal-bonded CO is 1.158 Å, with the small cluster, and 1.154 Å, with the large one. For the bridge-bonded species, a distance of 1.183 Å with the small cluster, but a slightly lower value of 1.174 Å has been computed with the large one. The difference between these two values might be directly related to differences in CO vibrational frequencies. In the case of the adsorption at 4-fold hollow sites, a value of 1.204 Å has been obtained with the small cluster and 1.185 Å with the large one. The results using the large cluster agree very well with the values reported by Pacchioni et al. This is also found to be the case for the Pt−C distance.

3.2. CO on Pt{110}. In this section we will discuss results obtained for the adsorption of CO on the two possible sites of Pt{110}; a summary is presented in Table 2. As mentioned above, it is not appropriate to compare the binding energies calculated using different cluster models. Therefore, we will only refer to those calculated with the largest cluster model. For the terminal-bonded CO, the binding energy computed on the Pt_{29} representation of Pt{110} is 150 kJ/mol, much larger than the value obtained for the bridge-bonded CO which is of 68 kJ/mol. This large difference in binding energy is in agreement with the fact that adsorption of CO at bridge sites is not experimentally observed in the low coverage regime. We recall than Bare et al.[32] assigned to bridge-bonded CO species a peak observed in HREELS experiments but only for coverages ranging from 0.5 to 0.9. This seems to indicate that adsorption of CO at bridge sites on Pt{110} is largely unfavored compared to adsorption at on-top sites in agreement with present calculations. Moreover, the binding energy predicted for the adsorption of CO at on-top sites also using the Pt_{29} cluster model is in close agreement with the 150 kJ/mol value estimated by Engstrom and Weinberg[34] and by Fair and Madix.[28] However, a larger value, 183 ± 7 kJ/mol, has been recently by Wartnaby et al.[35] from microcalorimetric measurements. Given the limitations of the cluster model approach, the agreement with experiment is rather remarkable. The value predicted by a modest Pt_{29} representation of Pt{110} is only ∼15% in error with respect to sophisticated microcalorimetric measurements in ultrahigh vacuum conditions which already have a ∼4% error bar.

For the vibrational frequencies we will discuss results obtained from both, small and large, cluster models of Pt{110}. The calculated values for the CO stretching vibration mode corresponding to chemisorption on the on-top and bridge sites obtained from the small cluster models are 2109 and 1941 cm^{-1}, respectively. As in the cases discussed in the previous section, the values predicted with the large cluster are not significantly different from those obtained using the smaller model. In fact, the values predicted from Pt_{29} are 2082 and 1933 cm^{-1}, respectively. Moreover, these calculated values are very similar to those obtained from different experiments. At low coverage, the HREELS experiments reported by Bare et al.[32] exhibit a well-defined peak at 2080 cm^{-1}, attributed to terminal-bonded CO, and only at rather high coverage do the experiments, exhibit a new feature at 1915 cm^{-1}, assigned to the bridge-bonded CO stretching frequency. We shall remind that, at coverages higher than 0.5, the 1 × 2 reconstruction is completely removed.[30−32] Further, Klunker et al.[26] observed a band at 2088 cm^{-1}, ascribed to the terminal-bonded CO stretching frequency. Depending on the experimental conditions, this band appears at 2065 cm^{-1} and was assigned to CO on-top of the Pt{110}-(1 × 2) reconstructed surface. We must point out that Klunker et al. did not observed any band in the region between 1850 and 1950 cm^{-1}, even at high exposure. While we cannot comment on the peak appearing at 2065 cm^{-1}, the remaining assignments are fully consistent with present calculations. Finally, we note that the different experiments aimed to give information about vibration modes do also show a band at 485 cm^{-1}[32] or at 472 cm^{-1}[126] attributed to the terminal-bonded metal−CO stretching, or frustrated translational, frequency. With the large cluster model, the calculated frequency for the metal−CO stretching vibration mode is 459 cm^{-1}, close enough to the experimental values. The different experimental techniques were not able to detect any band that could be assigned to the frustrated translation of the CO in the bridge site. This is surely due to the very low frequency at which this band would appear, our theoretical estimate being of ∼343 cm^{-1} (Table 2).

The discussion about the adsorption of CO on Pt{110} will be completed by examining the calculated geometrical parameters. Unfortunately, comparison with experiment is not possible because of the lack of experimental data. First, we notice that the terminal-bonded CO distance as well as the bridge-bonded CO distance are quite similar to those reported in the previous section for Pt{100}. For the small cluster model, the terminal-bonded CO distance is 1.153 Å and remains almost unchanged, 1.155 Å (when using the largest cluster model, the bridge-bonded CO distance is 1.172 Å for the small cluster and 1.179 Å for the large cluster. Noticeable, albeit small, differences arise in the perpendicular distance from CO to the surface in the case of the bridge-bonded species. For adsorption on Pt{100} the calculated value, for the large cluster, was 1.490 Å whereas the corresponding value for Pt{110} is 1.451 Å. In the case of adsorption at on-top sites, the metal−CO distance calculated for Pt{110} is almost the same previously found for Pt{100}. Therefore, only small differences appear when comparing the structural parameters of CO on Pt{100} and on Pt{110} surfaces.

3.3. CO on Pt{111}. The results obtained for the adsorption of CO on the Pt{111} surface are summarized in Table 3. Once again, we will only comment the binding energies calculated by using the largest cluster model. The binding energy for the adsorption of CO at on-top sites is 110 kJ/mol, whereas a much lower value, 24 kJ/mol, is obtained for the adsorption at bridge

sites. The difference in binding energy between the two adsorption sites agrees with the fact that bridge-bonded species are only observed when increasing coverage.[17,18] Our results are in good concordance with values estimated by several authors using different techniques. A value of 117 kJ/mol was reported by Ertl et al.[9] from desorption measurements; a similar value, 118 kJ/mol, was reported by Burghaus and Conrad from molecular beam relaxation spectroscopy. On the other hand, microcalorimetric experiments carried out by Yeo et al.[27] suggest a rather larger value of 183 kJ/mol. Again, the calculated value is of the order of the experimental value but lower than the one arising from the most recent and accurate measurements.

For CO at the on-top site, the calculated vibrational frequencies for the large (small) models are 2098 (2081) cm^{-1} for the CO stretching mode and 409 (472) cm^{-1} for the metal−CO stretching frequency. Corresponding values for CO at the bridge site are 1860 (1874) and 379 (415) cm^{-1}, respectively. IRAS experiments carried out by Hayden et al.[18] show the appearance of two bands. The first one appears at 2094 cm^{-1} and was assigned to adsorption at on-top sites. The second band is very broad and was resolved into two different peaks, the lowest one at 1810 cm^{-1}, attributed to adsorption of CO at high coordinate sites, and the second one, in the region between 1840 and 1857 cm^{-1}, attributed to adsorption at bridge sites. Our results seems to support some of the assignments of the vibrational spectra suggested by Hayden et al.[18] Steininger et al.[17] observed a band at 2100 cm^{-1}, in EELS experiments, attributed to terminal-bonded CO stretching frequency, and a second band at 480 cm^{-1} attributed to the metal−CO stretching frequency. When increasing coverage they also observed two additional bands, one at 1850 cm^{-1} and the second at 380 cm^{-1}, these bands were attributed to CO stretching frequency and metal−CO stretching frequency, for CO molecules adsorbed at bridge sites, respectively. Again, the large cluster model has given the results which are more comparable to the experimental values. Other IRAS experiments by Hoge et al.[21,23] report three bands, one at 2104 cm^{-1}, a second one at 1855 cm^{-1}, and the third one at 467 cm^{-1}. These bands are associated with the terminal-bonded CO stretching frequency, the bridge-bonded CO stretching frequency, and the terminal-bonded metal−CO stretching frequency, respectively. A more recent study by Klünker et al.,[26] using the sum frequency generation, obtained a value of 2082.7 ± 1.8 cm^{-1} for the stretching CO at on-top sites, and 1853.7 ± 2.0 cm^{-1} for the molecules adsorbed at bridge sites. The present theoretical results are in enough good agreement with the experimental values. Again, the ab initio cluster model approach appears as a reliable approach to the description of the adsorption of molecules on metal surfaces.

Finally, we will compare the geometrical parameters calculated for the adsorption of CO on Pt{111} with those reported by Ogletree et al.[20] from by quantitative LEED analysis. The CO equilibrium distance for the terminal-bonded species reported by Ogletree et al. is 1.15 Å and the same value was assumed in the LEED analysis for the bridge-bonded species. The Pt−C distance obtained from LEED is 1.85 Å for the adsorption at on-top sites and 2.08 Å for the adsorption at bridge sites. The present calculated value is 1.152 (1.157) Å for the terminal-bonded CO equilibrium distance, calculated with the large (small) cluster model. These values for the adsorbed CO distance are in excellent agreement with that reported by Ogletree and support the hypothesis that CO distance is site insensitive. The calculated values for the Pt−C distance are 1.907 (1.852) Å for the adsorption at the on-top site and 2.003 (1.955) Å for the adsorption at the bridge site. Again, the values calculated in this work are in good agreement with the LEED assignments.

4. Analysis of the Bonding Mechanism

The adsorption of CO to metal surfaces is usually described in terms of the Blyholder model.[73] Using a simple Hückel molecular orbital approach, Blyholder proposed that a σ-bond is formed between the CO, via the carbon atom, and a metal atom, and that further bonding is provided by the partial filling of the $2\pi^*$-antibonding CO molecular orbital. This bonding model of σ-donation and π-back-donation has since been widely accepted. However, one must realize that it is essentially a qualitative model that cannot explain all fine details of bonding. The Blyholder model is perhaps too simplistic, but it is believed to contain the main contributions that describes the CO−metal surface bonding. In fact, Hoffmann and co-workers argued that a major deficiency of the Blyholder model is to not take into account the 4σ CO molecular orbital.[74−76] However, a recent study carried out by Hu et al.[77] concluded that 4σ- and 1π-CO-molecular orbitals are mixed with the metal d-bands, but the levels arising from this interaction were found to lie well below the metal Fermi level, E_F, and hence, their net contribution to the chemisorption energy was predicted to be very small. Therefore, the 5σ- and $2\pi^*$-CO-molecular orbitals, which are strongly mixed with metal bands, are the responsible for the net bonding to the surface. Rangelov et al.[36] concluded, from photemission experiments, that the bond in the case of Pt{110} has a markedly 5σ donor character.

The validity of the Blyholder model for CO on Pt(111) has been also studied in detail by means of different theoretical techniques[63,64] following the procedure previously used by Bagus and co-workers for CO on other metal surfaces.[78−83] Bagus et al. used the constrained space orbital variation, CSOV, technique to decompose the interaction energy of CO and a surface cluster model and have shown that the substrate polarization and the π-back-donation play an important role in the bonding formation. The metal surfaces studied by Bagus et al. involved completely filled d-shells, and hence, σ-donation could not make a large contribution. Bagus and co-workers added a new contribution that was not considered yet. This important contribution to the bonding formation involves the Pauli repulsion between the frozen densities of the interacting fragments. In subsequent works, Bagus et al. used the CSOV technique to decompose the vibrational frequency shifts and shown that the Pauli repulsion plays a very important role, this is the "wall effect" leading to an increase of the CO stretching frequencies which is compensated by other mechanisms. Despite this large body of evidence, Onishi and Watari[60] claimed that for the adsorption of CO on Pt{111} there is no significant bonding contribution arising from the π-back-donation mechanism. A careful analysis of CO on Pt{111}, also based in the CSOV technique, has shown that π-back-donation is indeed the most important bonding contribution.[63] The CSOV analysis of the vibration frequency of CO on Pt{111} also brought new important and unexpected information.[64] The Blyholder model for bonding of CO on metal surfaces also attempts to explain the observed vibration shifts. In particular, it assumes that σ-donation increases the CO vibration frequency, because the adsorbed CO molecule acquires some CO^+ character and that π-back-donation contributes to the red shift because CO acquires CO^- character. The CSOV analysis by Illas et al.[64] has shown that both σ-donation and π-back-donation contribute to the red shift and that the only blue shift contribution arises from the "wall effect" identified by Bagus et al.[78−80] We shall demon-

TABLE 4: Analysis of the Bonding Mechanism by Means of the CSOV Technique: Binding Energy (B.E.) Decompositions for CO Chemisorbed at On-Top Sites and Those for CO Chemisorbed at Bridge Sites (Energies Are in kJ/mol)[a]

1. On-Top Sites

		Pt{100}		Pt{110}		Pt{111}	
n	CSOV step	B.E.	B.E.$_n$−B.E.$_{n-1}$	B.E.	B.E.$_n$−B.E.$_{n-1}$	B.E.	B.E.$_n$−B.E.$_{n-1}$
1	frozen orbital	−342		−509		−286	
2	cluster polarization	−166	176	−270	239	−147	139
3	back-donation	−4	162	−116	154	9	155
4	CO polarization	19	23	−93	23	33	24
5	donation	130	111	14	107	144	111
6	HF	159	29	40	25	172	28
7	B3LYP	178	19	139	99	229	57

2. Bridge Sites

		Pt{100}		Pt{110}		Pt{111}	
n	CSOV step	B.E.	B.E.$_n$−B.E.$_{n-1}$	B.E.	B.E.$_n$−B.E.$_{n-1}$	B.E.	B.E.$_n$−B.E.$_{n-1}$
1	frozen orbital	−596		−565		−536	
2	cluster polarization	−288	308	−258	308	−326	210
3	back-donation	−23	265	−19	238	−69	257
4	CO polarization	15	39	16	36	−36	34
5	donation	151	136	133	117	91	126
6	HF	189	38	163	30	123	32
7	B3LYP	244	55	168	5	126	4

[a] B.E.$_n$−B.E.$_{n-1}$ is the contribution of the *n*th step to the binding energy.

strate that, for the adsorption of CO on low index platinum surfaces, π-back-donation is an important contribution to the bonding formation and that σ-donation cannot be ignored.

We will study the bonding mechanism of CO on the Pt low index surfaces by using again the CSOV method supplemented by the analysis of orbital occupancies arising from a projection technique.[83,84] Before entering into the discussion of the results, let us briefly recall the main features of these two theoretical methods for the analysis of the bond. The CSOV method allows to decompose the binding energy into several contributions; the first contribution accounts for the Pauli repulsion, the second one corresponds to the substrate polarization, and next there is the surface to CO donation (mainly the π-back-donation contribution) followed by CO polarization and CO to surface donation (mainly σ-donation). The CSOV decomposition thus described has been carried out at the Hartree−Fock level of theory at the final B3LYP geometries. Since all other calculations reported in the present paper have been carried out at the B3LYP level, which implicitly includes electronic correlation effects, we consider an additional step in the energy decomposition by taking into account the electronic correlation effects estimated from the difference between B3LYP and Hartree−Fock energies. On the other hand, the projection technique allows us to measure the extent to which an orbital is contained in a many electron wave function as the expectation value of the proper orbital projection operator. The analysis reported in this section corresponds to the small cluster models. This choice does not affect the final conclusion since recent work[64] for CO on Pt{111} has shown that the relative importance of the different contribution is not sensitive to the size of the cluster selected to represent a given surface.

The results of the analysis of the bonding are summarized in Tables 4 and 5. The results of the CSOV analysis for CO at on-top sites of the three low index surfaces considered in the present work are reported in Table 4.1. An important result from this systematic study is that, for this site, the contribution of

TABLE 5: CO Molecular Orbital Population for CO Chemisorbed at On-Top and Bridge Sites

1. On-Top Sites

orbital	Pt{100}	Pt{110}	Pt{111}
1σ	2.000	2.000	2.000
2σ	2.000	2.000	2.000
3σ	1.999	2.000	2.000
4σ	1.997	1.997	1.997
1π	3.993	3.992	3.994
5σ	1.595	1.513	1.604
2π*	0.662	0.649	0.646
charge	−0.245	−0.151	−0.240

2. Bridge Sites

orbital	Pt{100}	Pt{110}	Pt{111}
1σ	2.000	2.000	2.000
2σ	2.000	2.000	2.000
3σ	2.000	2.000	2.000
4σ	1.993	1.994	1.992
1π	3.977	3.981	3.980
5σ	1.290	1.276	1.294
2π*	0.956	0.929	0.948
charge	−0.216	−0.180	−0.214

the π-back-donation is almost the same for the three surfaces: 162 kJ/mol for Pt{100}, 154 kJ/mol for Pt{110}, and 156 kJ/mol for Pt{111}. This is consistent with a variation of the 5d Mulliken population of the Pt atoms of the active site which upon CO adsorption becomes ∼8.80, whereas before adsorption the 5d Mulliken population is of ∼8.98, although given the approximate nature of the Mulliken population this result has to be regarded from a qualitative point of view. The same effect is found for the σ-donation contributions which are 111 kJ/mol for Pt{100}, 107 kJ/mol for Pt{110}, and 111 kJ/mol for Pt{111}. Hence, the donation and back-donation contributions are similar to the three surfaces. This conclusion can also be reached by inspecting the orbital projections reported in Table 5, part 1. The occupancies of the 5σ- and 2π*-molecular orbitals of adsorbed CO at the on top adsorption site measured by means of the projection technique are more or less the same for the three surfaces. In conclusion, all our results indicate that the importance of the σ-donation and π-back-donation is the same for the adsorption of CO on Pt{100}, Pt{110}, and Pt{111}. So far, these CSOV and orbital projection analyses do not permit to explain the origin of the differences in binding energy of CO on these low index surfaces. Clearly, the origin does not lie in the chemical σ-donation and π-back-donation mechanisms. Therefore, differences in substrate polarization and, more probably, differences in Pauli repulsion originated from the different topology of the surface conduction bands are responsible for the observed binding energies. We close this part by noting that results in Table 5 clearly show that 4σ and 1π CO molecular orbitals are not involved in the chemisorption bond.

Similar to the on top case, results for the adsorption of CO at bridge sites are summarized in Table 4, part 2 and 5, part 2. The description of the chemisorption bond that can be extract from these results is very similar to that described above. Again, the π-back-donation is quite similar for all the three surfaces, varying from 265 kJ/mol for Pt{100} to 239 kJ/mol for the Pt{110}. The σ-donation is also very similar for the three surfaces, exactly as in the case of adsorption at on-top sites. The values calculated for the contribution of σ-donation are 136 kJ/mol for Pt{100}, 117 kJ/mol for Pt{110}, and 127 kJ/mol for Pt{111}. The most important contribution is again π-back-donation. Moreover, we notice that the more important the π-back-donation the more important the σ-donation; this is the

TABLE 6: Analysis of the Vibrational Frequency by Means of the CSOV Technique for CO Chemisorbed at On-Top and Bridge Sites (Frequencies Are in cm^{-1}). ν_n-ν_{n-1} Is the Contribution of the *n*th Step to the CO Stretching Frequency

1. On-Top Sites

		Pt{100}		Pt{110}		Pt{111}	
n	CSOV step	ν	ν_n-ν_{n-1}	ν	ν_n-ν_{n-1}	ν	ν_n-ν_{n-1}
1	frozen orbital	2958	515[a]	3101	658	2856	413[a]
2	cluster polarization	2838	−120	2931	−170	2766	−90
3	back-donation	2511	−327	2595	−336	2478	−288
4	CO polarization	2477	−34	2573	−22	2454	−24
5	donation	2360	−117	2447	−126	2355	−99
6	HF	2271	−89	2386	−61	2297	−58
7	B3LYP	2064	−207	2109	−277	2081	−216

2. Bridge Sites

		Pt{100}		Pt{110}		Pt{111}	
n	CSOV step	ν	ν_n-ν_{n-1}	ν	ν_n-ν_{n-1}	ν	ν_n-ν_{n-1}
1	frozen orbital	2768	325[a]	2660	217[a]	2742	299[a]
2	cluster polarization	2652	−116	2548	−112	2616	−126
3	back-donation	2296	−356	2233	−315	2264	−352
4	CO polarization	2276	−20	2204	−29	2239	−25
5	donation	2179	−97	2120	−84	2146	−94
6	HF	2049	−130	2079	−41	2042	−103
7	B3LYP	1881	−168	1941	−138	1874	−168

[a] Frequency shift respect to the calculated free CO stretching frequency.

well-known synergetic effect. Again, cluster polarization and Pauli repulsion effects are important contributions. Finally it is interesting to compare the adsorption at on-top sites to the adsorption at bridge sites. The π-back-donation is significantly larger in the second case, but the σ-donation remains more or less the same, being always slightly larger for the bridge site. This difference in π-back-bonding is supposed to be responsible for the different CO stretching frequencies of CO molecules adsorbed at on-top sites and at bridge sites. This will be discussed at length in the forthcoming section.

5. Analysis of the Vibration Frequencies

Following the strategy earlier suggested by Bagus at al.,[78−80] we have also employed the CSOV method to study the effect of the different bonding mechanisms, introduced at the various CSOV steps, on the CO stretching frequency ν_{CO} as a function of the crystal face and of the surface site. The CSOV decomposition of ν_{CO} has been carried out at the Hartree−Fock level and the final result compared with the B3LYP value. The Hartree−Fock values for the absolute values of the vibrational frequency are usually largely overestimated and, hence, cannot be directly compared to experiment. However, this is a rather systematic deviation and the shift between adsorbed and the free CO $\Delta\nu_{CO}$ is qualitatively well described. Moreover, this analysis has been carried out using the small cluster models only; this choice is justified from the results on section 3 which show that the vibrational frequency for the CO internal stretching is rather independent of the surface model.

Overall, the decomposition of the CO frequency follows the trends already found for the case of terminal-bonded CO on Pt(111),[63,64] thus supporting the general validity of these previous analysis. In fact, from the summary of results collected in Table 6, parts 1 and 2. we notice that the superposition of the frozen electronic densities always produces a very large blue shift with respect to the ν_{CO} value for the gas-phase molecule. This result has already been described by Bagus et al.[78−80] and is the result of the Pauli repulsion on the vibrational frequency, evidencing the "surface wall" effect.[78−80] For CO adsorption at on-top sites, this blue shift is specially large: 515 cm^{-1} for Pt{100}, 658 cm^{-1} for Pt{110}, and 413 cm^{-1} for Pt{111}. While this shift is always large, the use of the relatively small cluster models does not permit to extract conclusions regarding the extent of Pauli repulsion on a given site on different crystal faces. However, it is possible to distinguish the effect on the different sites. In fact, the "wall effect" for the bridge sites is found to be 325 cm^{-1} for Pt{100}, 217 cm^{-1} for Pt{110}, and 299 cm^{-1} for Pt{111}. The clear difference between on-top and bridge sites is a clear consequence of the decrease on electronic density at the bridge site as compared to the atop one.

All the remaining bonding mechanisms contribute to decrease the "wall effect" on ν_{CO}, the π-back-donation being the leading term. We must point out that a large part of the electronic correlation effect, estimated as difference between HF and B3LYP values, does also contribute to the π-back-donation mechanism. Contrarily to the Pauli repulsion, the importance of π-back-donation in decreasing the initial ν_{CO} frequency is quite similar for the adsorption at on-top sites and at bridge sites. The values for the terminal- and bridge-bonded CO on Pt{100} are −327 and −356 cm^{-1}; the difference between these two values is small and cannot be used to differentiate the two sites. It must be pointed out that, at first sight, this is a rather surprising result because the contribution of the π-back-donation to the interaction energy is always larger for the bridge sites by $\sim$ 100 kJ/mol. However, in relative terms, the π-back-donation contribution is always $\sim$30% of the total energy recovered from the frozen orbital description. The situation for Pt{110}is also the same and a somehow larger difference appear in the case of the {111} surface. However, the differences are not large enough to claim that a differential effect exists. The fact that π-back-donation contribution to ν_{CO} is insensitive with respect to the crystal face is in full agreement with the CSOV decomposition of the interaction energy and orbital projection analysis discussed in the previous section. Next, we analyze the effect on $\Delta\nu_{CO}$ produced by the σ-donation mechanism. Notice that, in agreement with previous work[64] and contrary to what is assumed in the Blyholder mechanism, this bonding contribution does also contribute to the final red shift. Again, the differences appearing in this bonding mechanism between different sites and different faces is small enough to prevent further discussion. Similarly, we avoid discussing the substrate polarization effect because its contribution to $\Delta\nu_{CO}$ is clearly more sensitive to the particularities of the surface model used. Finally, we notice that the effect of electron correlation on ν_{CO} is of $\sim$200 cm^{-1}, independent of the adsorption site.

There is an important and new conclusion emerging from the previous analysis regarding the differences in the vibrational frequency of CO adsorbed on different sites. The sum of all contributions to the vibrational shift, substrate, and CO polarizations plus σ-donation and π-back-donation, overcome the initial "wall effect" and are thus responsible for the observed red shift. This is fully in agreement with previous studies for CO on several metal surfaces.[63,64,78−80] However, the origin of the differences on vibrational shift found for different sites largely arises from the differences in the initial Pauli repulsion or "wall effect". Therefore, the site differences on the inter- and intraunit bonding mechanisms are much smaller and can be ignored in a first-order approach. As a result, the Pauli repulsion, and not the chemical terms, is the responsible for the observed differences in vibrational frequencies at different sites. This does not mean that the chemical terms can be neglected to explain the final vibrational frequency, a blue shift will appear if only Pauli

repulsion is considered. Nevertheless, Pauli repulsion governs the difference between top and bridge sites.

Conclusions

In this work, a systematic theoretical study of the adsorption of CO on the Pt{100}, Pt{110}, and Pt{111} surfaces has been carried out by means of cluster model representations of the different surfaces and ab initio Hartree−Fock and hybrid B3LYP density functional theory calculations. The equilibrium geometries and vibrational frequencies have been found to be rather independent of the cluster model chosen to represent the surface, thus supporting the idea that these are local properties. For the interaction on the Pt{111} surface, the calculated values for equilibrium distances are in excellent agreement with those obtained from quantitative LEED analysis.[20] This agreement permits to suggest that the values obtained for the two other crystal faces constitute, in fact, accurate predictions for values not yet available from experimental measurements. The vibrational frequencies computed for different sites and for different crystal faces are also in good agreement with the experimental data. Contrary to what has been found for the equilibrium geometries and vibrational frequencies, the calculated interaction energies are found to be very sensitive to the surface cluster model. Nevertheless, for the most stable site, the use of the largest cluster models leads to interaction energies which are ∼80% of the recently reported microcalorimetric measurements.

The analysis of the chemisorption bond carried out by means of the CSOV and projection operator techniques reveals, once again, that the bonding interactions are dominated by the π-back-donation although σ-donation plays a significant role. From the energy CSOV decomposition, the contribution of π-back-donation to the chemisorption bond seems to be larger for the interaction at the bridge sites. However, the relative contribution for on-top and bridge sites, measured as the π-back-donation energy decrease divided by the sum of all contributions, is very similar. This is consistent with the CSOV analysis of the vibrational shift of chemisorbed CO. This analysis clearly shows that all bonding mechanisms contribute to reduce the initial blue shift caused by the "surface wall" effect. The π-back-donation contribution is essential to explain the final observed red shift. This is in agreement with previous work for CO on the Pt{111} surface. However, the π-back-donation contribution to the red shift is very similar for CO on on-top and bridge sites. Hence, π-back-donation cannot be the responsible for the observed difference for CO vibrational frequency on on-top and bridge sites. The CSOV decomposition reveals that the leading term contributing to this difference in ν_{CO} is the initial Pauli repulsion or "wall effect"; this is a new, important, and unexpected conclusion.

Acknowledgment. Financial support from the Spanish "Ministerio de Educación y Ciencia", Projects CICyT PB95-0847-C02-01 and CICyT PB95-0847-C02-02, and from "Generalitat de Catalunya" under Projects SGR97-167 and SGR97-17 is fully acknowledged. Part of the computer time was provided by the "Centre de Supercomputació de Catalunya", C^4-CESCA, through a research grant from the University of Barcelona. D. Curulla is grateful to the Universitat Rovira i Virgili for a predoctoral grant.

References and Notes

(1) Dry, M. E. In *Catalysis Science and Technology*; Anderson, J. R., Boudart, M., Eds.; Springer-Verlag: New York, 1981; Vol. 1.
(2) Vannice, M. A. In *Catalysis Science and Technology*; Anderson, J. R., Boudart, M., Eds.; Springer-Verlag: New York, 1982; Vol. 3.
(3) Taylor, K. C. In *Catalysis Science and Technology*; Anderson, J. R., Boudart, M., Eds.; Springer-Verlag: New York, 1984; Vol. 5.
(4) "New trends in CO activation." Stud. Surf. Sci. Catal. **1991**, *64*.
(5) Jones, J. H.; Kummer, J. T.; Otto, K.; Shelef, M.; Weaver, E. E. *Environ. Sci. Technol*. **1971**, *5*, 790.
(6) Shigeishi, R. A.; King, D. A. *Surf. Sci*. **1976**, *58*, 379.
(7) Bradshaw, A. M.; Hoffmann, F. W. *J. Catalysis* **1976**, *44*, 328.
(8) Crossley, A.; King, D. A. *Surf. Sci*. **1977**, *68*, 528.
(9) Ertl, G.; Neumann, M.; Streit, K. M. *Surf. Sci*. **1977**, *64*, 393.
(10) Froitzheim, H.; Hopster, H.; Ibach, H.; Lehwald, S. *Appl. Phys*. **1977**, *13*, 147.
(11) Hopster, H.; Ibach, H. *Surf. Sci*. **1978**, *77*, 109.
(12) Baro, A. M.; Ibach, H. *J. Chem. Phys*. **1979**, *71*, 4812.
(13) Crossley, A.; King, D. A. *Surf. Sci*. **1980**, *95*, 131.
(14) Avery, N. R. *J. Chem. Phys*. **1981**, *74*, 4202.
(15) Campbell, C. T.; Ertl, G.; Kuipers, H.; Segner, J. *Surf. Sci*. **1981**, *107*, 207.
(16) Campbell, C. T.; Ertl, G.; Segner, J. *Surf. Sci*. **1982**, *115*, 309.
(17) Steininger, H.; Lehwald, S.; Ibach, H. *Surf. Sci*. **1982**, *123*, 264.
(18) Hayden, B. E.; Bradshaw, A. M. *Surf. Sci*. **1983**, *125*, 787.
(19) Trenary, M.; Tang, S. L.; Simonson, R. J.; McFeely, F. R. *Surf. Sci*. **1983**, *124*, 555.
(20) Ogletree, D. F.; van Hove, M. A.; Somorjai, G. A. *Surf. Sci*. **1986**, *173*, 351.
(21) Hoge, D.; Tüshaus, M.; Schweizer, E.; Bradshaw, A. M. *Chem. Phys. Lett*. **1988**, *151*, 230.
(22) Olsen, C. W.; Masel, R. I. *Surf. Sci*. **1988**, *201*, 444.
(23) Schweizer, E.; Persson, B. N. J.; Tüshaus, M.; Hoge, D.; Bradshaw, A. M. *Surf. Sci*. **1989**, *213*, 49.
(24) Brandt, R. K.; Sorbello, R. S.; Greenler, R. G. *Surf. Sci*. **1992**, *271*, 605.
(25) Burghaus, U.; Conrad, H. *Surf. Sci*. **1995**, *331*−*333*, 116.
(26) Klünker, C.; Balden, M.; Lehwald, S.; Daum, W. *Surf. Sci*. **1996**, *360*, 104.
(27) Yeo, Y. Y.; Vattuone, L.; King, D. A. *J. Chem. Phys*. **1997**, *106*, 392.
(28) Fair, J.; Madix, R. J. *J. Chem. Phys*. **1980**, *73*, 3480.
(29) Jackman, T. E.; Davies, J. A.; Jackson, D. P.; Unertl, W. N.; Norton, P. R. *Surf. Sci*. **1982**, *120*, 389.
(30) Hofmann, P.; Bare, S. R.; Richardson, N. V.; King, D. A. *Solid State Commun*. **1982**, *42*, 645.
(31) Hofmann, P.; Bare, S. R.; King, D. A. *Surf. Sci*. **1982**, *117*, 245.
(32) Bare, S. R.; Hofmann, P.; King, D. A. *Surf. Sci*. **1984**, *144*, 347.
(33) Hayden, B. E.; Robinson, A. W.; Tucker, P. M. *Surf. Sci*. **1987**, *192*, 163.
(34) Engstrom, J. R.; Weinberg, W. H. *Surf. Sci*. **1988**, *201*, 145.
(35) Wartnaby, C. E.; Stuck, A.; Yeo, Y. Y.; King, D. A. *J. Phys. Chem*. **1996**, *100*, 12483.
(36) Rangelov, G.; Memmel, N.; Bertel, E.; Dose, V. *Surf. Sci*. **1991**, *251/252*, 965.
(37) Heilmann, P.; Heinz, K.; Müller, K. *Surf. Sci*. **1979**, *83*, 487.
(38) Barteau, M. A.; Ko, E. I.; Madix, R. J. *Surf. Sci*. **1981**, *102*, 99.
(39) Norton, P. R.; Davies, J. A.; Creber, D. K.; Sitter, C. W.; Jackman, T. E. *Surf. Sci*. **1981**, *108*, 205.
(40) Heinz, K.; Lang, E.; Strauss, K.; Müller, K. *Surf. Sci*. **1982**, *120*, L401.
(41) Behm, R. J.; Thiel, P. A.; Norton, P. R.; Ertl, G. *J. Chem. Phys*. **1983**, *78*, 7438.
(42) Thiel, P. A.; Behm, R. J.; Norton, P. R.; Ertl, G. *J. Chem. Phys*. **1983**, *78*, 7449.
(43) Hopkinson, A.; Guo, X.-C.; Bradley, J. M.; King, D. A. *J. Chem. Phys*. **1993**, *99*, 8262.
(44) Martin, R.; Gardner, R.; Bradshaw, A. M. *Surf. Sci*. **1995**, *342*, 69.
(45) Yeo, Y. Y.; Wartnaby, C. E.; King, D. A. *Science* **1995**, *268*, 1731.
(46) Yeo, Y. Y.; Vattuone, L.; King, D. A. *J. Chem. Phys*. **1996**, *104*, 3810.
(47) Ertl, G.; Norton, P. R.; Rüstig, J. *Phys. Rev. Lett*. **1982**, *49*, 177.
(48) Behm, R. J.; Thiel, P. A.; Norton, P. R.; Bindner, P. E. *Surf. Sci*. **1984**, *147*, 143.
(49) Uchida, Y.; Lehmpfuhl, G.; Imbihl, R. *Surf. Sci*. **1990**, *234*, 27.
(50) Uchida, Y.; Imbihl, R.; Lehmpfuhl, G. *Surf. Sci*. **1992**, *275*, 253.
(51) Hong, S.; Richarson, H. H. *J. Phys. Chem*. **1993**, *97*, 1258.
(52) Hopkinson, A.; King, D. A. *Chem. Phys*. **1993**, *177*, 433.
(53) Imbihl, R.; Ertl, G. *Chem. Rev*. **1995**, *95*, 697.
(54) Gruyters, M.; Ali, T.; King, D. A. *Chem. Phys. Lett*. **1995**, *232*, 1.
(55) Miners, J. H.; Martin, R.; Gardner, P.; Nalezinski, R.; Bradshaw, A. M. *Surf. Sci*. **1997**, *377*−*379*, 791.
(56) Ray, N. K.; Anderson, A. B. *Surf. Sci*. **1982**, *119*, 35.
(57) Gavezzotti, A.; Tantardini, G. F.; Simonetta, M. *Chem. Phys. Lett*. **1986**, *129*, 577.
(58) Smith, G. W.; Carter, E. A. *J. Phys. Chem*. **1991**, *95*, 2327.
(59) Roszak, S.; Balasubramanian, K. *J. Phys. Chem*. **1993**, *97*, 11238.
(60) Onishi, S.; Watari, N. *Phys. Rev. B* **1994**, *49*, 14619.

(61) Chung, S.-C.; Krüger, S.; Pacchioni, G.; Rösch, N. *J. Phys. Chem*. **1995**, *102*, 3695.
(62) Chung, S.-C.; Krüger, S.; Ruzankin, S. Ph.; Pacchioni, G.; Rösch, N. *Chem. Phys. Lett*. **1996**, *248*, 109.
(63) Illas, F.; Zurita, S.; Rubio, J.; Marquez, A. M. *Phys. Rev. B* **1995**, *52*, 12372.
(64) Illas, F.; Zurita, S.; Marquez, A. M.; Rubio, J. *Surf. Sci*. **1997**, *376*, 279.
(65) Illas, F.; Mele, F.; Curulla, D.; Clotet, A.; Ricart, J. M. *Electrochim. Acta* **1999**. In press.
(66) Philipsen, P. H. T.; van Lenthe, E.; Snijders, J. G.; Baerends, E. J. *Phys. Rev. B* **1997,** *56*, 13556.
(67) Pacchioni, G.; Chung, S.-C.; Krüger, S.; Rösch, N. *Surf. Sci*. **1997**, *392*, 173.
(68) Hay, P.; Wadt, W. R. *J. Chem. Phys*. **1985**, *82*, 299
(69) Zurita, S.; Illas, F.; Barthelat, J. C.; Rubio, J. *J. Chem. Phys*. **1996**, *104*, 8500.
(70) Dupuis, M.; Johnston, F.; Márquez, A. *HONDO 8.5 from CHEM-Station*; IBM Corporation: Kingston, 12401; 1994.
(71) Frisch, M. J.; Trucks, G. W.; Schlegel, H. B.; Gill, P. M. W.; Johnson, B. G.; Robb, M. A.; Cheeseman, J. R.; Keith, T.; Petersson, G. A.; Montgomery, J. A.; Raghavachari, K.; Al-Laham, M. A.; Zakrzewski, V. G.; Ortiz, J. V.; Foresman, J. B.; Peng, C. Y.; Ayala, P. Y.; Chen, W.; Wong, M. W.; Andres, J. L.; Replogle, E. S.; Gomperts, R.; Martin, R. L.; Fox, D. J.; Binkley, J. S.; Defrees, D. J.; Baker, J.; Stewart, J. P.; Head-Gordon, M.; González, C.; Pople, J. A. *Gaussian 94*, Revision B.3; Gaussian, Inc.: Pittsburgh, PA, 1995.
(72) Boys, S. F.; Bernardi, F. *Mol. Phys*. **1970,** *19*, 553.
(73) Blyholder, G. *J. Phys. Chem*. **1964**, *68*, 2772.
(74) Sung, S.-S.; Hoffmann, R. *J. Am. Chem. Soc*. **1985**, *107*, 578.
(75) Li, J.; Schiott, B.; Hoffmann, R.; Proserpio, D. M. *J. Phys. Chem*. **1990**, *94*, 1554.
(76) Wong, Y.-T.; Hoffmann, R. *J. Phys. Chem*. **1991**, *95*, 859.
(77) Hu, P.; King, D. A.; Lee, M. H.; Payne, M. C. *Chem. Phys. Lett*. **1995**, *246*, 73.
(78) Bagus, P. S.; Müller, W. *Chem. Phys. Lett*. **1985**, *115*, 540.
(79) Müller, W.; Bagus, P. S. *J. Vac. Sci. Technol. A* 1985, *3*, 1623.
(80) Bagus, P. S.; Pacchioni, G. *Surf. Sci*. **1990**, *236*, 233.
(81) Bagus, P. S.; Hermann, K.; Bauschlicher, C. W., Jr. *J. Chem. Phys*. **1984**, *80*, 4378.
(82) Bagus, P. S.; Hermann, K.; Bauschlicher, C. W., Jr. *J. Chem. Phys*. **1984**, *81*, 1966.
(83) Bagus, P. S.; Illas, F. *J. Chem. Phys*. **1992**, *96*, 8962.
(84) Nelin, C. J.; Bagus, P. S.; Philpott, M. R. *J. Chem. Phys*. **1987**, *87*, 2170.
(85) Whitten, J. L.; Yang, H. *Surf. Sci. Rep*. **1996**, *24*, 55.
(86) Bauschlicher Jr., C. W. *Chem. Phys. Lett*. **1986**, *129*, 586.
(87) Bagus, P. S.; Schaefer III, H. F.; Bauschlicher Jr., C. W. *J. Chem. Phys*. **1983**, *78*, 1390.
(88) Panas, I.; Schule, J.; Siegbahn, P. E. M.; Wahlgren, U. *Chem. Phys. Lett*. **1988**, *149*, 265.
(89) Ricart, J. M.; Rubio, J.; Illas, F.; Bagus, P. S. *Surf. Sci*. **1994**, *304*, 335.